Electrical Power Quality and Utilisation, Journal Vol. XI, No. 1, 2005

ANALYSIS OF OPERATION OF CLASS E ZVS RESONANT INVERTER

Elżbieta SZYCHTA
Technical University of Radom, Poland

***Summary*: The article discusses class E zero-voltage-switching resonant inverter (ZVS). The resonant circuit of the inverter is subject to mathematical analysis using the method of state variables with the aid of MATLAB software. Results of simulation testing, based on Simplorer software, of an inverter at the operating frequency of 100kHz are presented.**

Key words:
Class E ZVS resonant inverter
Output capacitance
MOSFET transistor
Zero-voltage-switching

1. INTRODUCTION

Demand for energy-saving converter systems of high operating frequencies led to development of resonant inverters where switching of semi-conductor power components occurs at zero voltage (ZVS) or zero current (ZCS) [1].

Designs of class E ZVS resonant inverters [3] include switches whose semi-conductor components are switched at zero voltage. A switch consists of a high switching frequency transistor, a discharging diode, and a resonant circuit that overloads at the inverter's operating frequency. The inverter's load is an element of the resonant circuit. Since the transistors are switched at zero voltage, class E ZVS inverters are the most efficient inverters known so far.

MOSFET power transistors enable inverters switching at frequencies of several MHz [5]. They are characterised by output capacitance of several hundred pF, which can be used in the process of switching of the transistors' operation as a component part of the resonant circuit [2].

Properties of resonant class E inverter including MOSFET transistor as its component part have been analysed, for instance, in [1, 3]. For purposes of the analysis, an ideal model of the transistor and ideal current source were assumed. A full mathematical model to comprise non-steady states was not provided, however. This article will discuss a class E ZVS resonant inverter, in consideration of the presence of resistance and the transistor output capacitance. A mathematical model of the circuit will be presented using equations of state variables. State variables will be analysed with the aid of MATLAB software. Results of simulation testing of the inverter based on Simplorer software will also be provided.

2. DESIGN AND OPERATION OF THE INVERTER

The circuit of the class E resonant inverter ZVS with one transistor switched at zero voltage is shown in Fig.1.

High-inductance choke L_d in series with the source of voltage E supplies current to the inverter. Power MOSFET T is switched at pulsation $\mathring{u}_T$. Backward diode D is an integral part of the transistor and enables bi-directional conductance of current i_S across the leg of the transistor. Inductance L, capacitance C, and load resistance R form a series resonant circuit. Capacitance $C1$ includes: parasitic capacitances of the choke L_d and of connections, as well as the parasitic output capacitance of the transistor T.

In the state of conducting, transistor T with resistance R_T ($R_T << R$) short-circuits capacitance $C1$. The series resonant circuit consists of: inductance L, capacitance C, load resistance R and transistor resistance R_T. Pulsation of ω_{01} of the resonant circuit R, R_T, L, C is given by:

$$\omega_{01} = \sqrt{\frac{1}{LC} - \left(\frac{R + R_T}{2L}\right)^2} \tag{1}$$

and the quality factor Q_{01} of the resonant circuit R, R_T, L, C is:

$$Q_{01} = \frac{\omega_{01} L}{(R + R_T)} = \frac{1}{\omega_{01} C (R + R_T)} \tag{2}$$

When transistor is off, the series resonant circuit comprises: inductance L, capacitances C and $C1$, and load resistance R. The capacitances C and $C1$ are in series, and the equivalent capacitance C_Z is lower than C and $C1$, and equals:

$$C_Z = \frac{CC1}{(C + C1)} \tag{3}$$

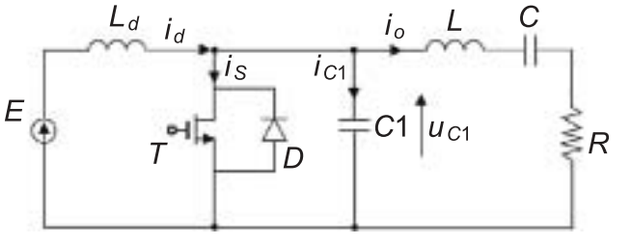

Fig.1. Class E ZVS resonant inverter

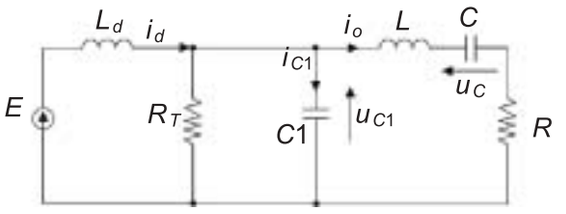

Fig. 2. Resonant circuit for the first interval of the inverter's operation

ω_{02} of the resonant circuit *R, L, C, C*1 is:

$$\omega_{02} = \sqrt{\frac{1}{LCC1/(C+C1)} - \left(\frac{R}{2L}\right)^2} \tag{4}$$

and the quality factor Q_{02} of the resonant circuit *R, L, C, C*1 is:

$$Q_{02} = \frac{\omega_{02} L}{R} = \frac{1}{\omega_{02} RCC1/(C+C1)} \tag{5}$$

The inverter can operate in three ranges which depend on the value of load resistance *R*:

— at $R = R_{opt}$ the inverter is in the range of optimum operation. The transistor is turned on and turned off at zero voltage, and turned on at zero current (soft commutation) [5].

— at $R < R_{opt}$ the inverter is in the range of suboptimum operation. The transistor is switched at zero voltage (soft commutation) and at hard current commutation. Power losses during transistor switching are greater than in the case of optimum operation, and the output power of the inverter is lower. The amplitude of load current is lower than in the case of optimum operation.

— at $R > R_{opt}$ the inverter is in the range of non-optimum operation. The transistor is turned on at hard voltage and current commutation, and turned off at zero voltage (soft commutation) and at hard current commutation. Power losses during transistor switching are greater than in the cases of optimum and sub-optimum operation.

3. ANALYSIS OF THE INVERTER'S RESONANT CIRCUIT

For purposes of the analysis, the following assumptions are made:

— The inverter is in the range of optimum operation, i.e. $R = R_{opt}$.

— The transistor on switch duty cycle *d* equals 0.5 [3].

— Transistor and the backward diode form a switch where the transistor on-resistance equals R_T, resistance of the backward diode during conducting is zero. Switching times of the switch are zero.

Analysis of the inverter's resonant circuit will be stated in relative units; base quantities of the voltage, current, and time are respectively: E, $E\omega_T C$, $1/\omega_T$.

$$\begin{cases} u^* = u(t)/E \\ i^* = i(t)/E\omega_T C \\ \tau = \omega_T t \end{cases} \tag{6}$$

where:

u^* — voltage in relative units,

i^* — current in relative units,

$u(t)$ — voltage as a function of time,

$i(t)$ — current as a function of time,

ω_T — operating pulsation of the transistor.

Cycle of the inverter's operation is divided into two intervals (Fig. 4). During the first interval: ($0 = \tau / \pi$) the transistor T is on.

Resonant circuit for the first interval of the operation, shown in Fig.2, is given by differential equations:

$$\begin{cases} u_{C1} = i_0 R + L\dfrac{di_0}{dt} + u_C \\ i_d = \dfrac{u_{C1}}{R_T} + i_0 + C1\dfrac{du_{C1}}{dt} \\ i_0 = C\dfrac{du_C}{dt} \\ E - L_d\dfrac{di_d}{dt} - u_{C1} = 0 \end{cases} \tag{7}$$

The system of equations (7) in relative units becomes:

$$\begin{cases} \dfrac{di_0^*}{d\tau} = \dfrac{1}{P_1 Q_1} u_{C1}^* - \dfrac{1}{Q_1} i_0^* - \dfrac{1}{P_1 Q_1} u_C^* \\ \dfrac{di_d^*}{d\tau} = \dfrac{1}{YP_1 Q_1} - \dfrac{1}{YP_1 Q_1} u_{C1}^* \\ \dfrac{du_{C1}^*}{d\tau} = \dfrac{1}{D} i_d^* - \dfrac{1}{P_2} u_{C1}^* - \dfrac{1}{D} i_0^* \\ \dfrac{du_C^*}{d\tau} = i_0^* \end{cases} \tag{8}$$

where:

$$\begin{cases} Q_1 = \dfrac{\omega_T L}{R}; \\ P_1 Q_1 = \omega_T^2 LC; \\ P_2 = \omega_T R_T C1 \\ D = \dfrac{C1}{C}; \\ Y = \dfrac{L_d}{L}; \end{cases} \tag{9}$$

Introducing designations of state variables:

$$\begin{cases} i_0^*(\tau) = x_1(\tau) \\ i_d^*(\tau) = x_2(\tau) \\ u_{C1}^*(\tau) = x_3(\tau) \\ u_C^*(\tau) = x_4(\tau) \end{cases} \tag{10}$$

and marking:

$$\begin{cases} a = \dfrac{1}{Q_1} \\ b = \dfrac{1}{P_1 Q_1} \\ c = \dfrac{1}{YP_1 Q_1} \\ d = \dfrac{1}{D} \\ e = \dfrac{1}{P_2} \end{cases} \tag{11}$$

equations of state are obtained:

$$\begin{cases} \dot{x}_1 = -ax_1 + bx_3 - bx_4 \\ \dot{x}_2 = -cx_3 + c \\ \dot{x}_3 = -dx_1 + dx_2 - ex_3 \\ \dot{x}_4 = x_1 \end{cases} \tag{12}$$

It is assumed that the initial conditions for the first interval are expressed by:

$$\begin{cases} i_0^*(0+) = x_1(0) = A_1^0 \\ i_d^*(0+) = x_2(0) = F_1^0 \\ u_{C1}^*(0+) = x_3(0) = B_1^0 \\ u_C^*(0+) = x_4(0) = G_1^0 \end{cases} \tag{13}$$

The system of equations (12) in the matrix form becomes:

$$\dot{\mathbf{X}}(\tau) = \mathbf{A_1} \cdot \mathbf{X}(\tau) + \mathbf{B_1} \cdot \mathbf{U}(\tau) \tag{14}$$

where:
$\mathbf{X}(\tau)$ — state vector
$\mathbf{U}(\tau)$ — input function
$\mathbf{A_1}$ — the system matrix for the first interval
$\mathbf{B_1}$ — control matrix for the first interval

$$\mathbf{X}(\tau) = \begin{bmatrix} x_1(\tau) \\ x_2(\tau) \\ x_3(\tau) \\ x_4(\tau) \end{bmatrix} \tag{15}$$

$$\mathbf{A_1} = \begin{bmatrix} -a & 0 & b & -b \\ 0 & 0 & -c & 0 \\ -d & d & -e & 0 \\ 1 & 0 & 0 & 0 \end{bmatrix}; \quad \mathbf{B_1} = \begin{bmatrix} 0 \\ c \\ 0 \\ 0 \end{bmatrix} \tag{16}$$

$$\mathbf{U}(\tau) = 1(\tau) \tag{17}$$

The vector of initial conditions $\mathbf{X_{01}}$ is:

$$\mathbf{X_{01}} = \begin{bmatrix} x_1(0) \\ x_2(0) \\ x_3(0) \\ x_4(0) \end{bmatrix} = \begin{bmatrix} A_1^0 \\ F_1^0 \\ B_1^0 \\ G_1^0 \end{bmatrix} \tag{18}$$

Applying Laplace transformation to the equation (14) and considering that $\tau = \omega_T t$, the following obtains:

$$s \cdot \frac{1}{\omega_T} \mathbf{X}\left(\frac{s}{\omega_T}\right) - \mathbf{X_{01}} = \mathbf{A_1} \cdot \frac{1}{\omega_T} \mathbf{X}\left(\frac{s}{\omega_T}\right) + \mathbf{B_1} \cdot \frac{1}{\omega_T} \cdot \mathbf{U}\left(\frac{s}{\omega_T}\right) \tag{19}$$

where:
s — Laplace operator.

Determining $\mathbf{\Phi}_1 = [s\mathbf{I} - \mathbf{A}_1]$, transform of the solution to the equation (14) becomes:

$$\mathrm{L}\left[\mathbf{X}(\tau)\right] = \mathbf{\Phi_1}^{-1} \cdot \left\{\mathbf{X_{01}} + \mathbf{B_1} \cdot \frac{1}{s}\right\} \tag{20}$$

where:
$\mathbf{I}$ — unit matrix,
$\mathbf{\Phi}_1{}^{-1}$ — reverse matrix of $\mathbf{\Phi}_1$:

$$\mathbf{\Phi_1} = \begin{bmatrix} s+a & 0 & -b & b \\ 0 & s & c & 0 \\ d & -d & s+e & 0 \\ -1 & 0 & 0 & s \end{bmatrix} \tag{21}$$

The determinant detΦ is a characteristic polynomial of the transform (20), and the equation:

$$M(s) = det\,\mathbf{\Phi_1} = 0 \tag{22}$$

is called a characteristic equation, whose roots decide the system's dynamics.

According to the equations (21) and (22), the characteristic polynomial $M(s)$ becomes:

$$M(s) = s^4 + a_3 s^3 + a_2 s^2 + a_1 s + a_0 \tag{23}$$

where:

$$\begin{cases} a_3 = a + e \\ a_2 = b + ae + bd + cd \\ a_1 = be + acd \\ a_0 = bcd \end{cases} \tag{24}$$

After applying (11) and (24), coefficients of the characteristic polynomial are produced as a function of parameters Q_1, P_1Q_1, P_2, Y, D:

$$\begin{cases} a_3 = \dfrac{1}{Q_1} + \dfrac{1}{P_2} \\ a_2 = \dfrac{1}{P_1Q_1} + \dfrac{1}{Q_1P_2} + \dfrac{1}{DP_1Q_1}\left(1 + \dfrac{1}{Y}\right) \\ a_1 = \dfrac{1}{P_1Q_1}\left(\dfrac{1}{P_2} + \dfrac{1}{YDQ_1}\right) \\ a_0 = \dfrac{1}{\left(P_1Q_1\right)^2 DY} \end{cases} \tag{25}$$

In the case of data assumed for purposes of simulation testing (p.4), which are defined in (9), the characteristic polynomial $M(s)$ in the equation (23) has two real roots, s_1 and s_2, and two complex conjugate roots, s_3 and s_4:

$$\begin{cases} s_1 = -\alpha \\ s_2 = -\beta \\ s_{3,4} = -\gamma \pm j\delta \end{cases} \tag{26}$$

therefore, the (23) can be represented by:

$$M(s) = (s+\alpha)(s+\beta)\left[(s+\gamma)^2 + \delta^2\right] \tag{27}$$

This form of characteristic polynomial is particularly important for determination of the state vector $\mathbf{X}(\tau)$. The values $\alpha, \beta, \gamma, \delta$ of the roots s_1, s_2, s_3, s_4 can be calculated using a number of software programmes, for instance, MATLAB or MAPLE.

The reverse matrix of $\mathbf{\Phi_1}$ is:

$$\mathbf{\Phi_1}^{-1} = \frac{1}{\Delta_1}\begin{bmatrix} s^2(s+e) + cds & bds \\ cds & (s+a)(s+e)s + b(s+e) + bds \\ -ds^2 & (s+a)ds + bd \\ s(s+e) + cd & bd \end{bmatrix} \tag{28}$$

$$\begin{bmatrix} bs^2 & -\{sb(s+e) + bcd\} \\ -\{(s+a)cs + bc\} & -bcd \\ (s+a)s^2 + bs & bds \\ bs & s(s+a)(s+e) + bds + cd(s+a) \end{bmatrix}$$

where: $\Delta_1 = det\,\mathbf{\Phi_1} = M(s)$.

In the first interval, the vector of initial conditions $\mathbf{X}_{01} = \mathbf{0}$, which means all its elements $A_1^0, F_1^0, B_1^0, G_1^0$ are zero. In view of the foregoing conditions and based on the (20), the equation (17) solves by:

$$\mathbf{X}(\tau) = L^{-1}\left\{\frac{1}{\Delta_1}\cdot\begin{bmatrix} \frac{c}{s}\cdot bds \\ \frac{c}{s}\cdot\{(s+a)(s+e)s + b(s+e) + bds\} \\ \frac{c}{s}\cdot\{(s+a)ds + bd\} \\ \frac{c}{s}\cdot bd \end{bmatrix}\right\} \tag{29}$$

After determining the original transform (29), state variables of the inverter are expressed by:

$$x_1(\tau) = A_1e^{-\alpha\tau} + B_1e^{-\beta\tau} + C_1e^{-\gamma\tau}\cos(\delta\tau) + \\ + \frac{D_1 - C_1\gamma}{\delta}e^{-\gamma\tau}\sin(\delta\tau) \tag{30}$$

$$x_2(\tau) = E_21(\tau) + A_2e^{-\alpha\tau} + B_2e^{-\beta\tau} + \\ + C_2e^{-\gamma\tau}\cos(\delta\tau) + \frac{D_2 - C_2\gamma}{\delta}e^{-\gamma\tau}\sin(\delta\tau) \tag{31}$$

$$x_3(\tau) = E_31(\tau) + A_3e^{-\alpha\tau} + B_3e^{-\beta\tau} + \\ + C_3e^{-\gamma\tau}\cos(\delta\tau) + \frac{D_3 - C_3\gamma}{\delta}e^{-\gamma\tau}\sin(\delta\tau) \tag{32}$$

$$x_4(\tau) = E_41(\tau) + A_4e^{-\alpha\tau} + B_4e^{-\beta\tau} + \\ + C_4e^{-\gamma\tau}\cos(\delta\tau) + \frac{D_4 - C_4\gamma}{\delta}e^{-\gamma\tau}\sin(\delta\tau) \tag{33}$$

The constant coefficients $A_1 - A_4$, $B_1 - B_4$, $C_1 - C_4$, $D_1 - D_4$, $E_2 - E_4$ in the expressions (30) – (33) depend on the values of a, b, c, d, e as defined in the equations (11), and on the roots $\alpha, \beta, \gamma, \delta$ of the characteristic polynomial (27). They can be determined by analytical methods, using e.g. MAPLE 9 application.

The dependencies (30), (31), (32), (33) give a mathematical description of state variables of: load current i_0^*, source current i_d^*, voltage u_{C1}^* capacitance $C1$ and voltage u_C^* of the capacitor C in the first interval of the resonant inverter ope-

ration. The first operating interval finishes when $\tau = \pi$. Transistor T stops conducting, voltage $u_{C1}^{*} = 0$, and the circuit continues on to the second operating interval.

The second interval of the inverter's operation: ($\pi < \tau \leq 2\pi$) begins the moment transistor T stops conducting.

The resonant circuit for the second interval, shown in Figure 3, is described by differential equations:

$$\begin{cases} L\dfrac{di_0}{dt} + u_C + i_0 R - u_{C1} = 0 \\ i_d = C1\dfrac{du_{C1}}{dt} + i_0 \\ i_0 = C\dfrac{du_C}{dt} \\ E - L_d\dfrac{di_d}{dt} - u_{C1} = 0 \end{cases} \tag{34}$$

The system of equations (34) in relative units becomes:

$$\begin{cases} \dfrac{di_0^*}{d\tau} = \dfrac{1}{P_1Q_1}u_{C1}^* - \dfrac{1}{P_1Q_1}u_C^* - \dfrac{1}{Q_1}i_0^* \\ \dfrac{di_d^*}{d\tau} = \dfrac{1}{P_1Q_1Y} - \dfrac{1}{P_1Q_1Y}u_{C1}^* \\ \dfrac{du_{C1}^*}{d\tau} = \dfrac{1}{D}i_d^* - \dfrac{1}{D}i_0^* \\ \dfrac{du_C^*}{d\tau} = i_0^* \end{cases} \tag{35}$$

Introducing state variables (10), (11), equations of state for the second interval are following:

$$\begin{cases} \dot{x}_1 = -ax_1 + bx_3 - bx_4 \\ \dot{x}_2 = -cx_3 + c \\ \dot{x}_3 = -dx_1 + dx_2 \\ \dot{x}_4 = x_1 \end{cases} \tag{36}$$

The system of equations (36) in the matrix form becomes:

$$\dot{\mathbf{X}}(\tau) = \mathbf{A_2}\cdot\mathbf{X}(\tau) + \mathbf{B_2}\cdot\mathbf{U}(\tau) \tag{37}$$

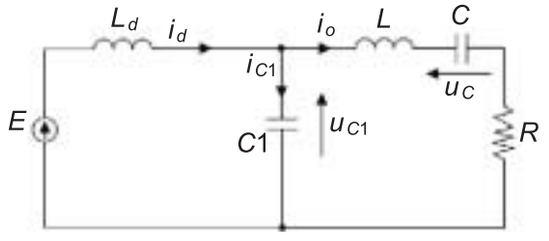

Fig. 3. Resonant circuit for the second interval of the inverter's operation

The system matrix $\mathbf{A}_2$ and the control matrix $\mathbf{B}_2$ become:

$$\mathbf{A_2} = \begin{bmatrix} -a & 0 & b & -b \\ 0 & 0 & -c & 0 \\ -d & d & 0 & 0 \\ 1 & 0 & 0 & 0 \end{bmatrix}; \quad \mathbf{B_2} = \begin{bmatrix} 0 \\ c \\ 0 \\ 0 \end{bmatrix} \tag{38}$$

The vector of initial conditions $\mathbf{X_{02}}$ is defined by:

$$\mathbf{X_{02}} = \begin{bmatrix} i_0^*(\pi) \\ i_d^*(\pi) \\ u_{C1}^*(\pi) \\ u_C^*(\pi) \end{bmatrix} = \begin{bmatrix} x_1(\pi) \\ x_2(\pi) \\ x_3(\pi) \\ x_4(\pi) \end{bmatrix} = \begin{bmatrix} A_2^0 \\ F_2^0 \\ B_2^0 \\ G_2^0 \end{bmatrix} \tag{39}$$

After transforming the equation (37), the dependence results:

$$s\cdot\frac{1}{\omega_T}\mathbf{X}\left(\frac{s}{\omega_T}\right) - \mathbf{X_{02}} = \mathbf{A_2}\cdot\frac{1}{\omega_T}\mathbf{X}\left(\frac{s}{\omega_T}\right) + \mathbf{B_2}\cdot\frac{1}{\omega_T}\cdot\mathbf{U}\left(\frac{s}{\omega_T}\right) \tag{40}$$

and hence the solution — the original vector $\mathbf{X}(\tau)$ is:

$$\mathbf{X}(\tau) = L^{-1}\left[\mathbf{\Phi_2}^{-1}\cdot\left\{\mathbf{X_{02}} + \mathbf{B_2}\cdot\frac{1}{s}\right\}\right] \tag{41}$$

In the event, the matrix $\mathbf{\Phi_2}$ is given by:

$$\mathbf{\Phi_2} = [s\mathbf{I} - \mathbf{A_2}] = \begin{bmatrix} s+a & 0 & -b & b \\ 0 & s & c & 0 \\ d & -d & s & 0 \\ -1 & 0 & 0 & s \end{bmatrix} \tag{42}$$

The characteristic polynomial $M(s)$ in this interval is expressed by:

$$M(s) = det\,\mathbf{\Phi_2} = s^4 + b_3s^3 + b_2s^2 + b_1s + b_0 \tag{43}$$

where:

$$\begin{cases} b_3 = a \\ b_2 = b + bd + cd \\ b_1 = acd \\ b_0 = bcd \end{cases} \tag{44}$$

After applying (11) and (44), coefficients of the characteristic polynomial are produced as a function of the parameters Q_1, P_1Q_1, P_2, Y, D:

$$\begin{cases} b_3 = \dfrac{1}{Q_1} \\ b_2 = \dfrac{1}{P_1 Q_1} + \dfrac{1}{DP_1 Q_1} + \dfrac{1}{DYP_1 Q_1} \\ b_1 = \dfrac{1}{Q_1} \cdot \dfrac{1}{DYP_1 Q_1} \\ b_0 = \dfrac{1}{\left(P_1 Q_1\right)^2 DY} \end{cases} \tag{45}$$

For the data assumed for purposes of simulation testing (p.4), as defined in the dependencies (9), the characteristic polynomial $M(s)$ defined in (43) has two pairs of complex conjugate roots:

$$\begin{cases} s_{1,2} = -m \pm jn \\ s_{3,4} = -p \pm jq \end{cases} \tag{46}$$

Hence, the expression (43) can be given by:

$$M(s) = \left[\left(s+m\right)^2 + n^2\right]\left[\left(s+p\right)^2 + p^2\right] = \Delta_2 \tag{47}$$

The reverse matrix Φ_2^{-1} of Φ_2, described in (42), becomes:

$$\boldsymbol{\Phi}_2^{-1} = \frac{1}{\Delta_2}\begin{bmatrix} s^3 + cds & bds & bs^2 & -s^2 b - bcd \\ cds & (s+a)s^2 + bs + bds & -(s+a)cs - bc & -bcd \\ -ds^2 & (s+a)ds + bd & (s+a)s^2 + bs & bds \\ s^2 + cd & bd & bs & (s+a)s^2 + bds + cd(s+a) \end{bmatrix} \tag{48}$$

On the basis of (41), the system of equations (36) solves by:

$$\mathbf{X}(\tau) = L^{-1}\left\{\frac{1}{\Delta_2}\begin{bmatrix} A_2^0 \cdot \left(s^3 + cds\right) + bd\left(F_2^0 s + c\right) + \\ + B_2^0 bs^2 - G_2^0\left(s^2 b + bcd\right) \\ A_2^0 cds + \left(F_2^0 s + c\right)\left[s(s+a) + b(1+d)\right] - \\ - B_2^0\left[(s+a)sc + bc\right] - G_2^0 bcd \\ \frac{1}{s}\left\{\begin{matrix} -A_2^0 ds^3 + \left(F_2^0 s + c\right)\left[(s+a)ds + bd\right] + \\ + B_2^0 s^2\left[s(s+a) + b\right] + G_2^0 bds^2 \end{matrix}\right\} \\ \frac{1}{s}\left\{\begin{matrix} A_2^0 s\left(s^2 + cd\right) + \left(F_2^0 s + c\right)bd + B_2^0 bs^2 + \\ + G_2^0 s\left[(s+a)s^2 + bds + cd(s+a)\right] \end{matrix}\right\} \end{bmatrix}\right\} \tag{49}$$

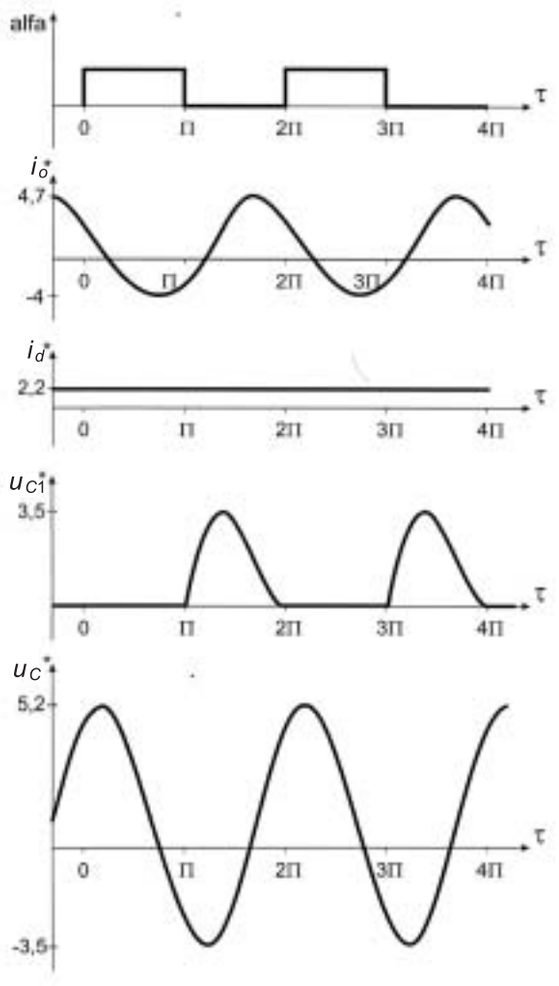

Fig. 4. Current and voltage waveforms, in relative units, during optimum (steady) operation of the inverter

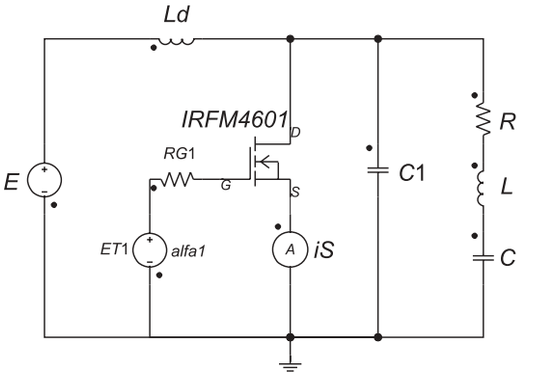

Fig. 5. Simulation model of the inverter

Table 1. Electrical parameters of the transistor MOSFET IRFM460 [7].

parameter		symbol	value	unit
drain-to-source voltage		u_{DS}	500	V
drain-to-gate voltage		u_{GS}	20	V
current between the drain and source	DC	i_D	19	A
	puls	i_{DM}	76	A
drain-to-source resistance		R_{DS}	0,27	Ω
input capacitance		C_{iss}	4300	pF
output capacitance		C_{oss}	1000	pF
switch times	upward slope of current I_D	t_r	120	ns
	delay of turn-on	$t_{d(on)}$	35	ns
	downward slope of current I_D	t_f	98	ns
	delay of turn-off	$t_{d(off)}$	130	ns

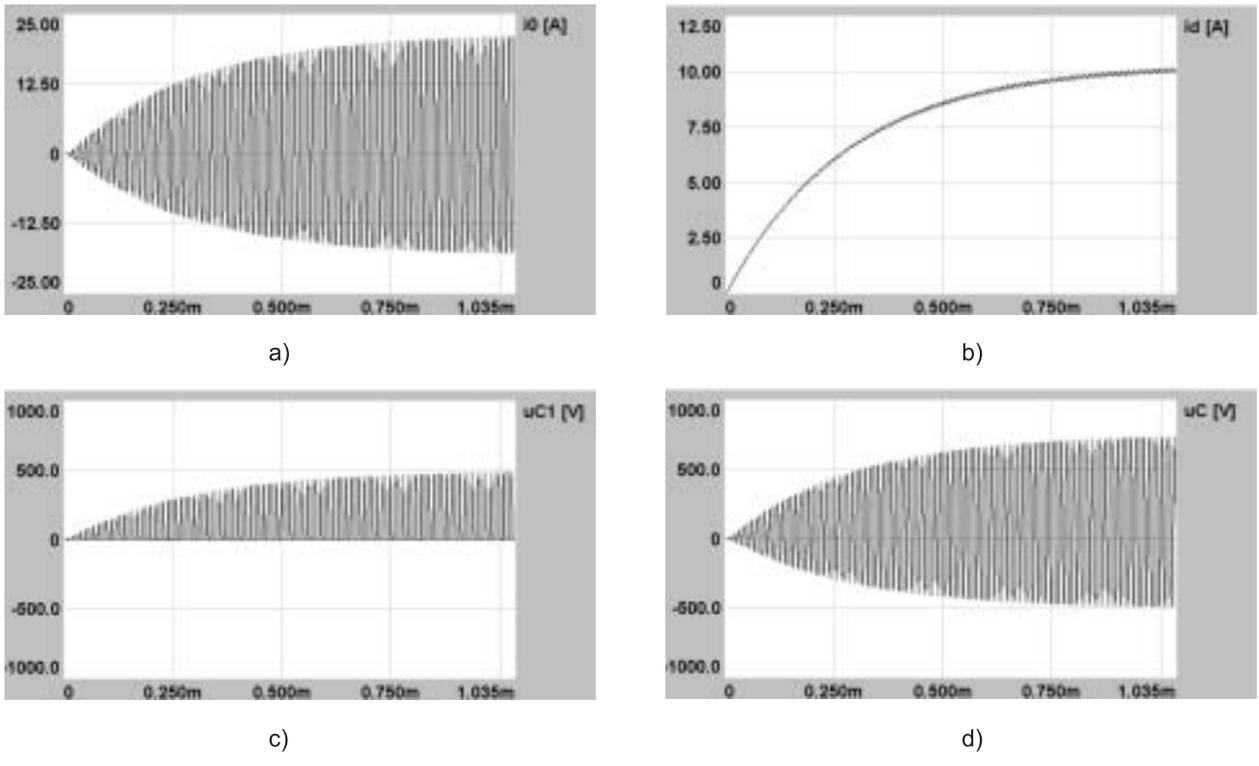

Fig.6. Current and voltage waveforms during the inverter's start-up generated from simulation; R = 6.7Ω, optimum operation; a) load current i_0, b) supply current i_d, c) voltage u_{C1} across transistor T, d) voltage u_C across capacitance C

After determining the original transform (49), the system's state variables are expressed by:

$$x_1(\tau) = A_1 e^{-m\tau}\cos n\tau + \frac{B_1 - mA_1}{n} e^{-m\tau}\sin n\tau + \\ + C_1 e^{-p\tau}\cos q\tau + \frac{D_1 - C_1\gamma}{q} e^{-p\tau}\sin q\tau \tag{50}$$

$$x_2(\tau) = A_2 e^{-m\tau}\cos n\tau + \frac{B_2 - mA_2}{n} e^{-m\tau}\sin n\tau + \\ + C_2 e^{-p\tau}\cos q\tau + \frac{D_2 - pC_2}{q} e^{-p\tau}\sin q\tau \tag{51}$$

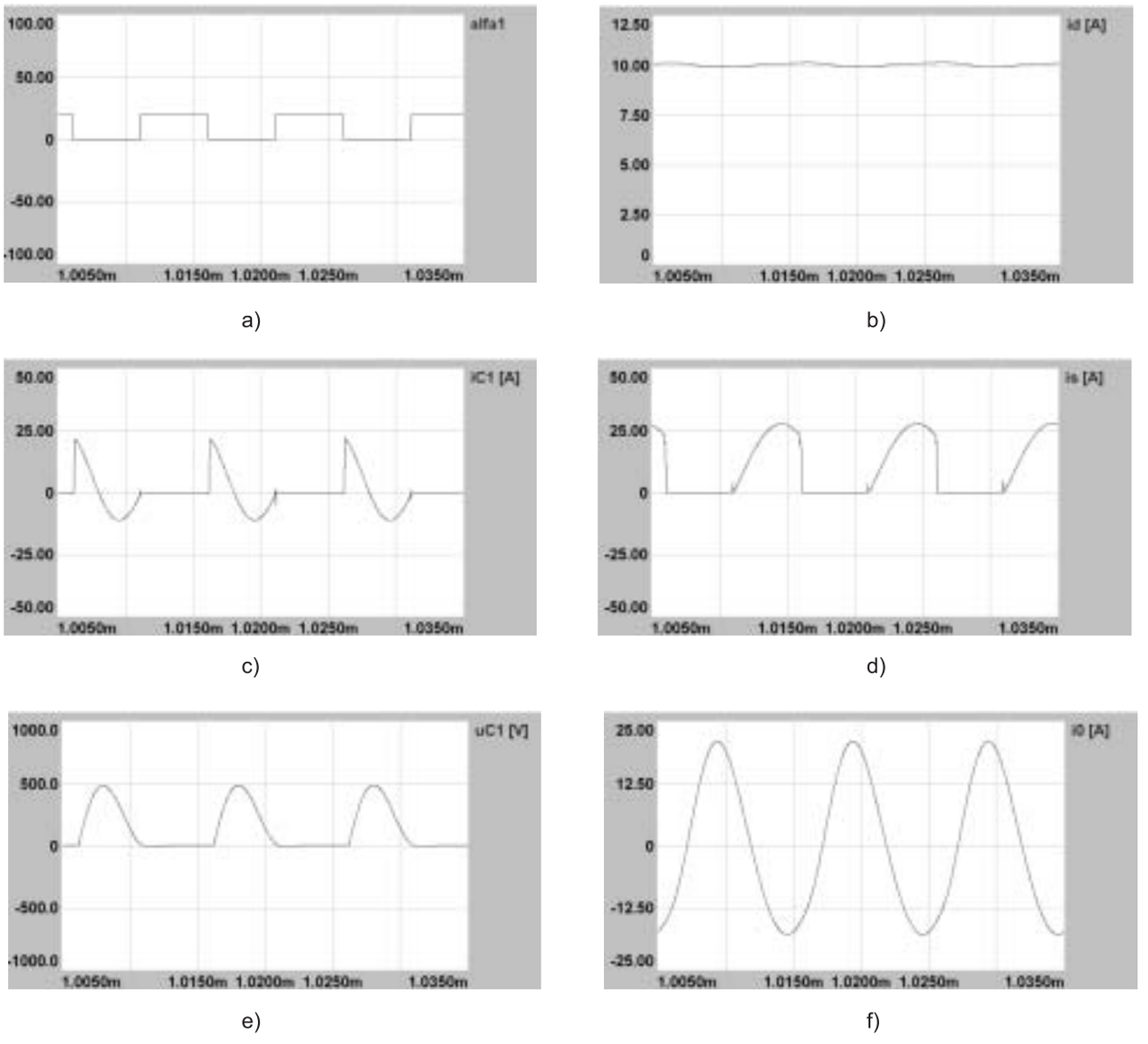

Fig.7. Current and voltage waveforms generated from simulation; R = 6.7Ω, optimum operation; a) control pulsation, b) supply current i_d, c) current i_{C1} of capacitance $C1$, d) current i_S in the transistor T leg, e) voltage u_{C1} across capacitance $C1$ or voltage u_T across transistor T, f) load current i_0

$$x_3(\tau) = E_3 1(\tau) + A_3 e^{-m\tau}\cos n\tau + \frac{B_3 - mA_3}{n} e^{-m\tau}\sin n\tau + \\ + C_3 e^{-p\tau}\cos q\tau + \frac{D_3 - pC_3}{p} e^{-p\tau}\sin q\tau \tag{52}$$

$$x_4(\tau) = E_4 1(\tau) + A_4 e^{-m\tau}\cos n\tau + \frac{B_4 - mA_4}{n} e^{-m\tau}\sin n\tau + \\ C_4 e^{-p\tau}\cos q\tau + \frac{D_4 - pC_4}{p} e^{-p\tau}\sin(q\tau) \tag{53}$$

The coefficients $A_1 - A_4$, $B_1 - B_4$, $C_1 - C_4$, $D_1 - D_4$, $E_3 - E_4$ from (50) – (53) depend on the values of a, b, c, d as defined in the system of equations (11), and on the roots m, n, p, q of the polynomial (47). Like in the first interval, they can be determined using MAPLE 9 software.

The dependencies (50), (51), (52), (53) are a mathematical description of the state variables of: load current i_0^*, source current i_d^*, voltage u_{C1}^* capacitance $C1$, and voltage u_C^* of the capacitor C in the second interval of the inverter operation.

Waveforms in subsequent cycles of the inverter's operation are determined in a way analogous to the method applied in the first cycle. The final conditions of the successive operation cycle become the initial conditions for the following cycle of the inverter's operation.

Current and voltage waveforms in the inverter, in relative units, during the inverter steady operation, as based on (31) – (33) and (50) – (53), are illustrated in Figure 4.

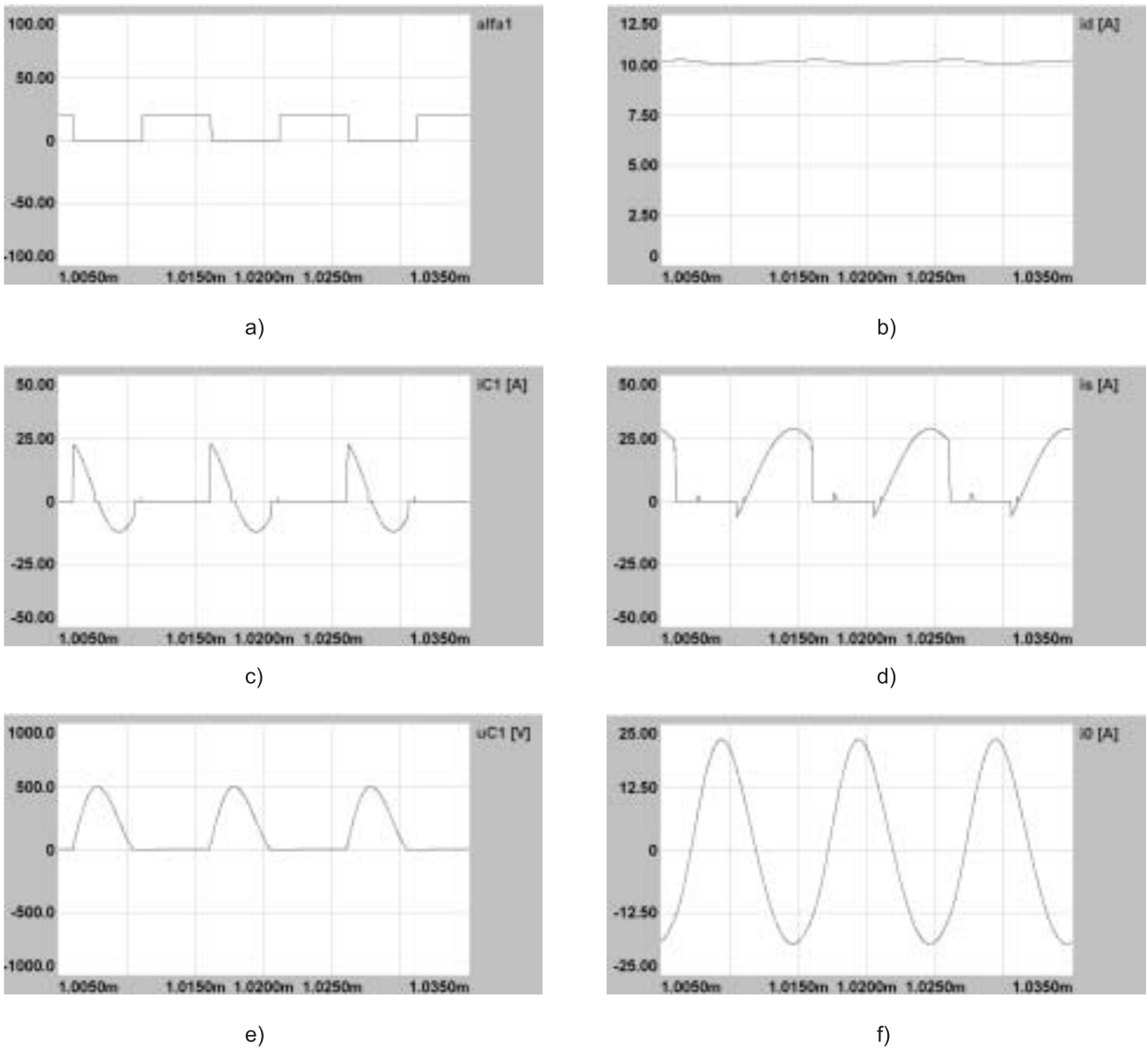

Fig. 8. Current and voltage waveforms in the inverter generated from simulation; R = 6Ω, suboptimum operation; a) control pulsation, b) supply current i_d, c) current i_{C1} of capacitance $C1$, d) current i_S in the transistor T leg, e) voltage u_{C1} across capacitance $C1$ or voltage u_T across transistor T, f) load current i_0

4. SIMULATION TESTS OF THE INVERTER

The resonant inverter was subject to simulation testing based on Simplorer software. The following data were assumed for purposes of designing the circuit: load power P_0 = 1000W, supply current I_d = 10A, Q_0 = 7, operating frequency of the inverter f_T = 100kHz, circuit efficiency η = 0.93, the transistor on switch duty cycle d = 0.5. According to [1], the circuit of the resonant inverter contains elements with the following values: L = 64.3μH, C = 50.7nF, $C1$ = 47.1nF, L_d = 3.8mH, E = 141.3V, R = var, as shown in Figure 5. The simulation tests were conducted for three operating ranges of the inverter, depending on the assumed values of the load resistance R. The simulation circuit comprised a MOSFET transistor IRFM460 produced by International Rectifier, whose parameters are described in Table 1. To calculate capacitance $C1$, the value of the transistor's output capacitance C_{oss} = 1000pF was considered.

Figure 6 shows current and voltage waveforms during start-up of the inverter at optimum operation. Inverter is switched at zero voltage u_{C1} across the transistor. The circuit is turned on smoothly, current and voltage waveforms tend towards the state of steady operation over a time proportional to the value of inductance L_d. Increasing value of L_d extends the start-up time, decreasing value of L_d raises pulsation of the source current i_d of the inverter. Sufficiently great inductance L_d produces a constant value of the inverter's supply current i_d during its steady operation.

Figures 7, 8, 9 illustrate current and voltage waveforms occurring in the inverter in the three ranges of the inverter's operation, which depend on the value of load resistance R. The inverter operates in a continuous way at frequencies of 100kHz. Operating pulsation of the inverter is greater than the pulsation of the resonant circuit R, L, C. In effect, the load becomes inductive in nature during the inverter operation.

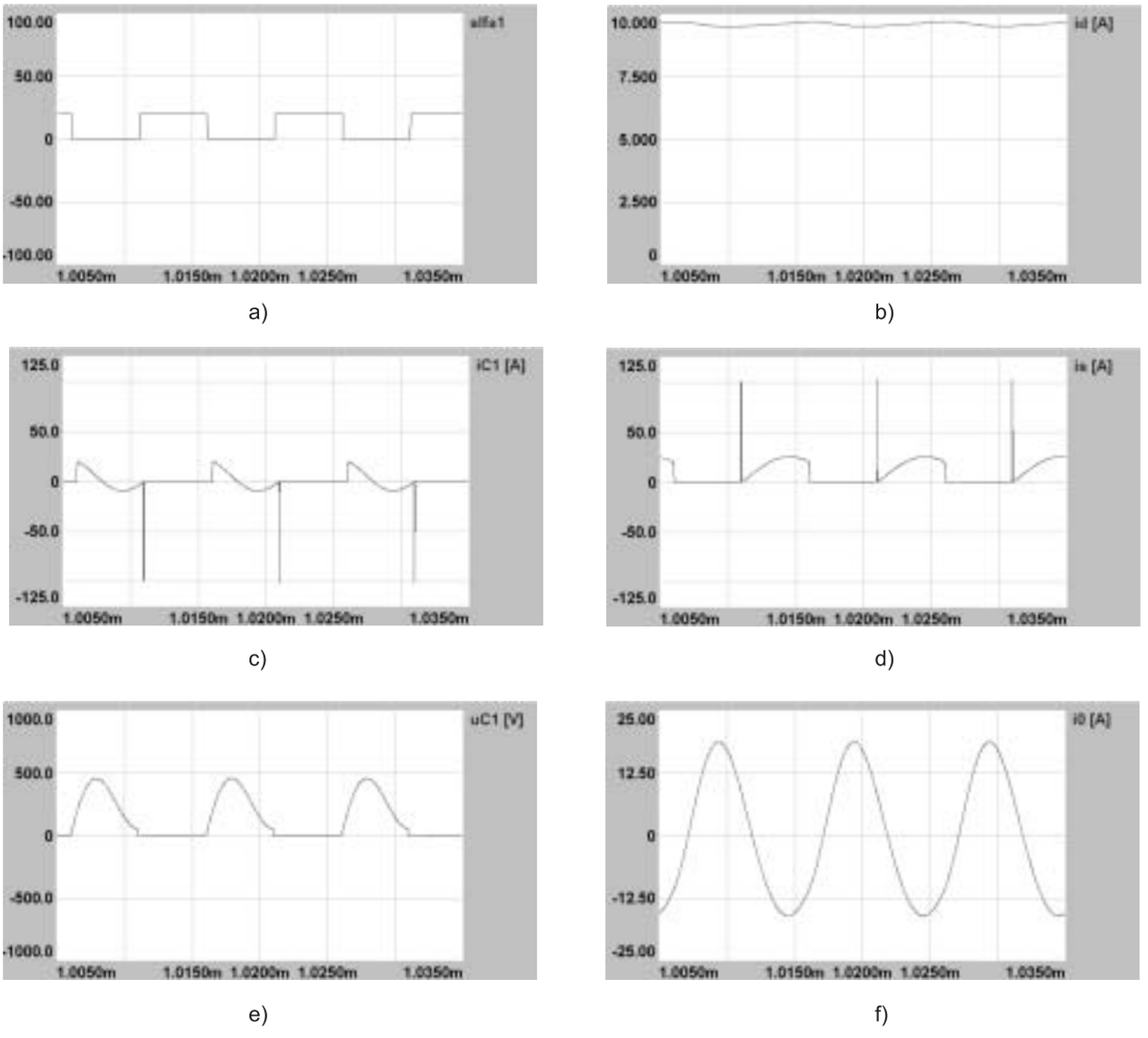

Fig. 9. Current and voltage waveforms in the inverter generated from simulation; R = 8Ω, non-optimum operation; a) control pulsation, b) supply current i_d, c) current i_{C1} of capacitance $C1$, d) current i_S in the transistor T leg, e) voltage u_{C1} across capacitance $C1$ or voltage u_T across transistor T, f) load current i_0

Shape of the resonant load current i_0 depends on the quality of the circuit. A high quality factor Q allows for a sinusoidal shape of the load current i_0.

Maximum values of voltages u_{C1} across the transistor T are about four times greater than the supply voltage E.

Figure 7 shows the optimum inverter operation at the load resistance $R = R_{opt}$. The transistor is turned on and off at zero voltage $u_{C1,}$ and turned on at zero current i_S. Analysis of the waveforms in Figure7 confirms that the optimum operation reduces switching power losses, thus providing for high efficiency and high frequency of the inverter's operation.

There is only one set of parameters: L, C, $C1$, L_d, R, where optimum operation is implemented at a given on switch duty cycle d of the inverter.

If the value of load resistance R is lower than the value of optimum resistance R_{opt}; $R < R_{opt}$, the inverter is in the range of sub-optimum operation, as presented in Figure 8. The transistor is turned on at zero voltage u_{C1} and at hard current commutation i_S. Diode D takes over the current i_S "accelerating" the transistor's turn on. Switching power losses are greater than in the case of optimum operation, and the inverter's output power is lower. The lower the value of resistance R, the higher the maximum value of voltage u_{C1} across the transistor.

If the value of load resistance R is higher than the value of optimum resistance $R_{opt;}$ $R > R_{opt}$ the inverter works in the range of non-optimum work, as presented in Figure 9. The transistor is turned on at hard commutation of voltage u_{C1} and of the current $i_{S,}$ and turned off at zero voltage u_{C1} and hard commutation of the current $i_{S.}$ Turn on occurs at the positive voltage u_{C1}, which produces a peak of the transistor's current i_S and increases power losses during the transistor's switching. Amplitude of the load current in the range of non- optimum operation is lower than the amplitude of the load current in the range of optimum operation.

CONCLUSION

The mathematical analysis and simulation tests of the inverter lead to the following conclusions:

— A precise mathematical model was developed. The results of simulation tests in the range of optimum operation confirm the results of theoretical analysis.
— The results of simulation tests confirm that the transistor is switched on and off at non-zero current in the range of suboptimum operation, and at non-zero voltage and current in the range of non-optimum operation. In the event, switching losses occur in the inverter.
— When the transistor is on, its output capacitance cooperates with the resonant capacitance and the circuit does not generate parasitic oscillations. When the diode is on, the transistor's output capacitance and resonant inductance generate parasitic oscillations. The maximum operating pulsation at which class E operation is achievable is limited by the output capacitance of the transistor.
— In the optimum operation interval, the transistor is switched at zero voltage and turned on at zero current, which reduces power losses at switching to a virtual zero.
— The peak voltage across the transistor is about four times higher than the input voltage. Therefore, the circuit is suitable for low input voltage applications.
— The optimum operation range is associated with one value of the load resistance at a given operating pulsation of the circuit. The inverter can also be in the suboptimum range of operation, but switching losses occur then, that are due to the hard current commutation.
— The inverter is very efficient and can be operated at high frequencies.

Researches should be continued to focus on real models in order to verify and confirm results of mathematical analysis and simulation testing in definite conditions of power supply and inverter load.

REFERENCES

1. Citko T., Tunia H., Winiarski B.: *Resonant Converters in Power Electronics.* Wydawnictwa Politechniki Białostockiej, Białystok 2001, (in Polish).
2. Januszewski S., Świątek H., Zymmer K.: *Semi-Conductor Power Equipment*. Warszawa. 1999, WKŁ, (in Polish).
3. Kazimierczuk M.K., Czarkowski D.: *Resonant Power Converters*. A Wiley-Intersience Publication. John Wiley and Sons. Inc. New York, Toronto, Singapure 1995,
4. Lin Y.L., Witulski, A.F.: *A unified treatment of a family of ZVS and ZCS resonant inverters*. Power Electronics Specialists Conference, 1997. PESC '97 Record., 28th Annual IEEE 1, 1997, p. 14–20.
5. Mikołajuk K.: *Fundamentals of Analysis of Power Electronic Circuits*. PWN, Warszawa 1998, (in Polish).
6. Szychta E.: *High Frequency Voltage Inverter with an Additional Resonant Circuit.* JUEE, 1/2, 10, 2004.
7. Szychta E.: *Resonant Inverter Powered by dc Voltage Source.* Automation and Control Technologies 2004, Proceedings of the V International Conference, Kaunas 2004, p. 26–30.
8. Szychta E.: *Impact of Output Capacitances of MOSFET-Type Transistors on the Operation of One-Phase Series Voltage Inverter*. Przegląd Elektrotechniczny, 4, 2005, (in Polish).
9. Tunia H., Barlik R.: *Theory of Converters.* 2nd Revised Edition. Warszawa, Oficyna Wydawnicza Politechniki Warszawskiej, 2003, (in Polish).
10. Web site: www.dialelec.com.

Elżbieta Szychta
Graduated from the Electrical Faculty of Warsaw Polytechnic in 1981. Obtained a degree of doctor of engineering from the Electrical Faculty of Warsaw Polytechnic in 1988. Since 1981 she has worked for the Transport Faculty Kazimierz Pulaski at the Technical University of Radom. An assistant professor in the Department of Electrical Machinery and Equipment. Interested in industrial power electronics.

Address: Politechnika Radomska, Wydział Transportu
26-600 Radom, ul. Malczewskiego 29; tel: (048) 361 77 00
e-mail: e.szychta@pr.radom.pl